

Soft chemical synthesis of nanosized zinc aluminate spinel from the thermolysis of different organic precursors

M. KUTTY PV¹, S. DASGUPTA^{1*}, S. BANDYOPADHYAY¹

¹ Ceramic Membrane Division, Central Glass & Ceramic Research Institute,
Council of Scientific & Industrial Research, Kolkata 700 032, India

A new method of preparation of nanocrystalline zinc aluminate (ZnAl_2O_4) powder is described in this paper. Different organic acids are used as template material and nitric acid as an oxidant. Single phase ZnAl_2O_4 spinel can be formed at a much lower temperature through this route which gives nanocrystalline powder with uniform particle size and morphology. The powders are characterized by thermo gravimetric analysis (TGA), X-ray diffraction analysis (XRD), Fourier transform infrared spectroscopy (FT-IR), BET surface area analysis and field emission scanning electron microscopy (FE-SEM). The average crystallite size of the single phase material was of 20 to 30 nm and the surface area was found to be 21 to 27 m^2g^{-1} .

Keywords: *solution evaporation, template, spinel, nanopowder*

© Wroclaw University of Technology.

1. Introduction

Zinc aluminate (ZnAl_2O_4) or gahnite, a naturally occurring spinel material, is widely used as ceramic, electronic and catalytic material [1]. As zinc aluminate is transparent to light with wavelengths above 320 nm, it is suitable for UV optoelectronic applications and thermal barrier coating for space craft [2–4]. Zinc aluminate is used as catalyst for dehydration of alcohols to olefins [5], synthesis of methanol and higher alcohols [6, 7], preparation of poly methyl benzene [8], synthesis of styrene from acetophenone [9], and double bond isomerization of alkenes [10]. It can also be used in ceramic tiles to improve wear resistance and mechanical properties [11].

Zinc aluminate powder has been prepared by many techniques such as solid-state [12], sol-gel [13], hydrothermal [14], micro emulsion [15], vacuum evaporation [16] and co-precipitation [17] methods. However, some of these processes are

either complex or expensive which limits their large scale production. Disadvantages of these methods are also the requirement of high temperature, inhomogeneity, lack of stoichiometry and low surface area. In general, high surface area is associated with smaller particle sizes for different catalytic and non catalytic applications. Hence, low temperature soft chemical synthesis of nanosized zinc aluminate particles has ample scope for application in different fields.

In this study we report on a new method of synthesis for ZnAl_2O_4 nanoparticles by an organic acid template route. Tartaric, oxalic and malic acids are used here as complexing agents and HNO_3 as an oxidising agent. The materials were characterized by TGA, FTIR, XRD, FESEM and BET surface area analysis.

2. Experimental procedures

All the chemicals used for the synthesis of ZnAl_2O_4 were of analytical grade (E. Merck). Deionized water was used for the preparation of all

*E-mail: sdasgupta@cgcri.res.in

solutions. ZnAl_2O_4 was synthesized by the following method:

2.975 g of (0.01 mole) zinc nitrate hexahydrate $[\text{Zn}(\text{NO}_3)_2 \cdot 6\text{H}_2\text{O}]$ and 7.52 g (0.02 mole) aluminium nitrate nonahydrate $[\text{Al}(\text{NO}_3)_3 \cdot 9\text{H}_2\text{O}]$ were dissolved in 2N nitric acid separately and then mixed together. 9 g (0.06 mole) tartaric acid dissolved in 50 ml of deionised water was added to it and the mixture was stirred continuously on a hot plate at its boiling temperature until all the liquid evaporated out of the solution. There was an evolution of brown fumes towards the end of the reaction leaving a fluffy grey mass. The green samples prepared were calcined at different temperatures to get single phase ZnAl_2O_4 spinel material. The synthesis was repeated with oxalic acid dihydrate and malic acid in place of tartaric acid, and the resultant powders were analyzed by different methods.

The samples were characterized using X-ray diffraction (Phillips PW 1710) using $\text{CuK}\alpha$ radiation, the powder morphology was studied using FESEM (supra 45 vp), thermal studies (TGA) were carried out using NETZSCH 409C analyzer, FTIR spectra studies were made with Nicolet Model 5PC FTIR. BET surface area analysis was carried out with Quantachrome instruments NOVA4000e.

3. Results

3.1. Tartarate Precursor Method

The XRD patterns of green and calcined (at different temperatures) powder synthesized via tartaric acid route are shown in Fig. 1. The XRD diffraction pattern of the synthesized green powder reveals that it is amorphous in nature. As the calcination temperature increases, the peaks become sharper, and the crystalline phase formation is completed at 600 °C. The XRD patterns are in excellent accordance with the powder data of JCPDS 05-0669 of zinc aluminate spinel. Characteristic high intensity peaks are observed at 36.906° due to the (3 1 1) plane (d-spacing 2.4436 Å), the next high peak at 31.321° is from the (2 2 0) plane (d spacing 2.8670 Å), other planes corresponding to peaks are denoted in the figure of calcined compounds. The

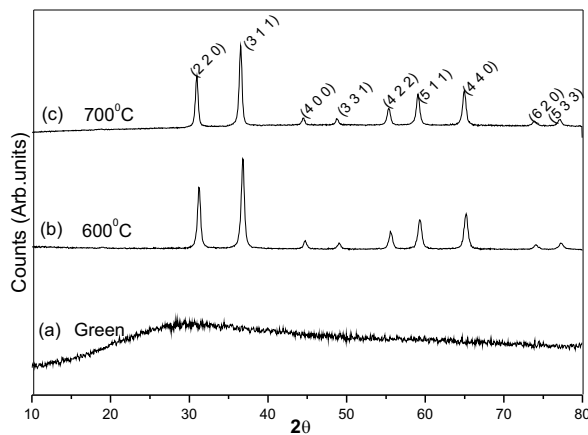


Fig. 1. XRD of the zinc aluminate powder (tartarate route) a) uncalcined, b) calcined at 600 °C and c) 700 °C.

average crystallite size (~ 30 nm) of the powders was calculated using Scherrer's equation (Eq. 1).

$$D = 0.9\lambda / \beta \cos \theta, \quad (1)$$

where D is the average grain size in nanometer, λ = X-ray wavelength (1.5406 Å) and β is the width of the diffraction peak at half maximum for the diffraction angle 2θ . Fig. 2 shows the FESEM micrographs of powder calcined at 700 °C (Tartarate route). Loosely aggregated extremely fine particles are observed. The crystallite size is in accordance with that obtained from XRD studies (30 nm). Surface area studies were carried out on a single phase material calcined at 700 °C. A high surface area of 21.07 m²/g was observed which indicates the formation of well crystallized nanosized material. Fig. 3 shows a TGA curve of the green synthesized powder up to 800 °C at a heating rate of 10 °C/min. The TGA graph shows a steady loss in weight up to 600 °C (about 10 %) which is due to the presence of trapped nitrates, residual carboxylate, unburned carbon and entrapped water. A slight loss in weight is observed from 600 °C to 800 °C (< 1%). The FTIR spectra recorded (400–4000 cm⁻¹) for green and calcined powders (at different temperatures) are shown in Fig. 4. The IR spectra of the green synthesized powder show a broad band around 3427 cm⁻¹ due to O–H of the co-ordinated water molecules [18]. The band at

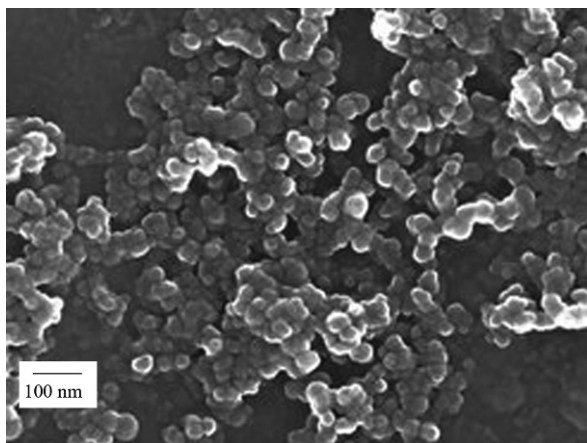


Fig. 2. FESEM micrographs of zinc aluminate powder (tartarate route) calcined at 700 °C.

1635 cm^{-1} is due to the bending mode of $\text{H}-\text{O}-\text{H}$ vibration [19]. The band in the zone between $1320\text{--}1400\text{ cm}^{-1}$ is attributed to $\text{C}=\text{O}$ of coordinated

COOH which is overlapped with an intense nitrate peak at 1376 cm^{-1} [20]. The broad peaks at 1096 cm^{-1} may correspond to the $\text{O}-\text{C}$ stretching for carboxylic acid. The peaks in the range of $400\text{--}700\text{ cm}^{-1}$ are difficult to interpret. Broad bands around 660 and 550 cm^{-1} become stronger with an increase in calcination temperature and correspond to the AlO_6 groups which build up ZnAl_2O_4 spinel and correspond to the formation of ZnAl_2O_4 spinel [21]. As the calcination temperature increases, the peaks due to $\text{O}-\text{H}$ and $\text{C}-\text{O}$ gradually disappear indicating the removal of impurities and formation of a single phase ZnAl_2O_4 spinel. Although XRD shows complete phase formation at 600 °C , FTIR studies indicate the presence of slight impurities due to the presence of occluded water and carbonaceous material. Hence, the powders were calcined up to 700 °C for subsequent studies.

3.2. Oxalate precursor method

The phase formation investigations using XRD (Fig. 5) were also carried out on uncalcined and calcined powders synthesized via oxalate route. As evidenced from the XRD, the green powder synthesized was amorphous in nature while after calcination at 600 °C single phase zinc aluminate spinel was formed. As described earlier the powder data

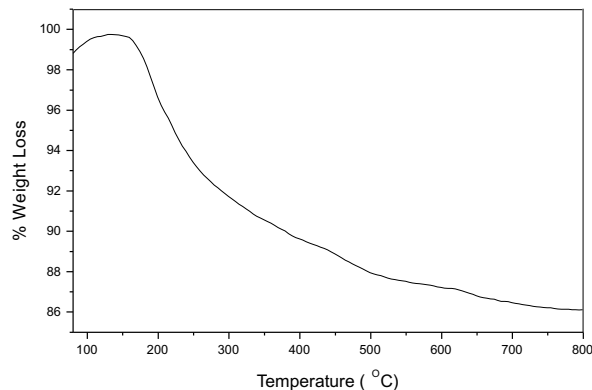


Fig. 3. TGA curve of the zinc aluminate precursor (tartarate route).

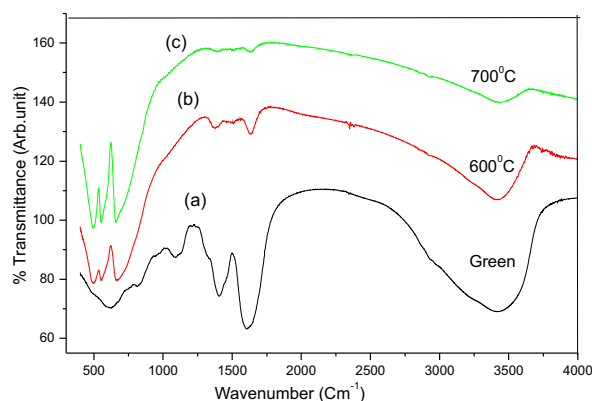


Fig. 4. FTIR spectra of zinc aluminate (tartarate route) a) uncalcined, b) calcined at 600 °C and c) 700 °C .

are in agreement with JCPDS 05-0669. The average crystallite size was calculated as 25 nm .

The FESEM micrograph of calcined powder (at 600 °C) is shown in Fig. 6. It shows agglomerated morphologies with average particle size of 30 nm . The BET surface area of the calcined powder was assessed as $25.37\text{ m}^2/\text{g}$.

The TGA curve of the green synthesized powder (oxalate route) up to 800 °C at a heating rate of $10\text{ °C}/\text{min}$ is shown in Fig. 7. A weight loss of about 5% is observed up to 630 °C followed by a sharp 6% weight loss from 630 °C to 700 °C .

FTIR spectra of synthesized green and calcined powders (Fig. 8) show major peaks of organic remnants. The peak of AlO_6 at 660 and 550 cm^{-1} is not seen in the spectra of green powder. As

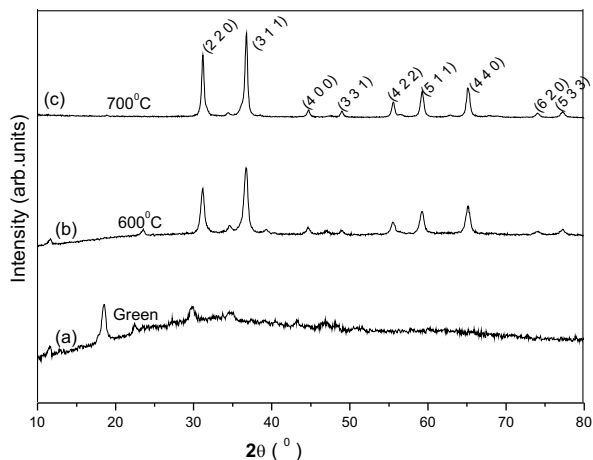


Fig. 5. XRD of the zinc aluminate powder (oxalate route) a) uncalcined, b) calcined at 600 °C and c) 700 °C.

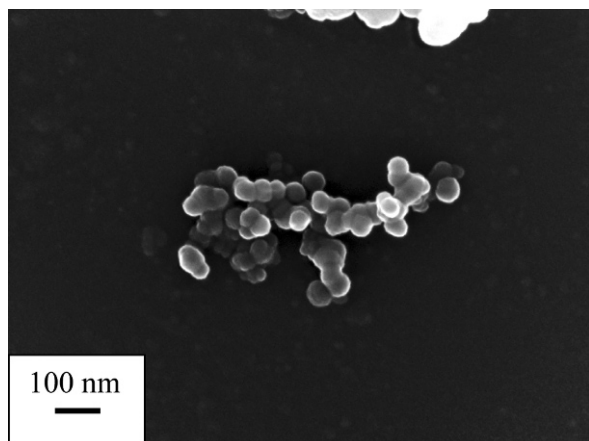


Fig. 6. FESEM micrographs of zinc aluminate powder (oxalate route) calcined at 700 °C.

the calcination temperature increases, the peaks due to water molecules and carbonaceous matters gradually disappear while the peak of AlO_6 appears and becomes stronger and sharper [21]. The peaks at 3431 cm^{-1} , 1629 cm^{-1} , 1376 cm^{-1} and 1096 cm^{-1} originate from hydroxyl group of lattice water molecule, bending mode of $\text{H}-\text{O}-\text{H}$ vibration, nitrate vibration, and $\text{O}-\text{C}$ of coordinated carboxylate respectively [18–20]. Similar to the tartrate method the XRD shows that the phase formation is completed at 600 °C, whereas the TGA and IR studies reveal that the impurities are eliminated completely at higher temperature, i.e. at 700 °C.

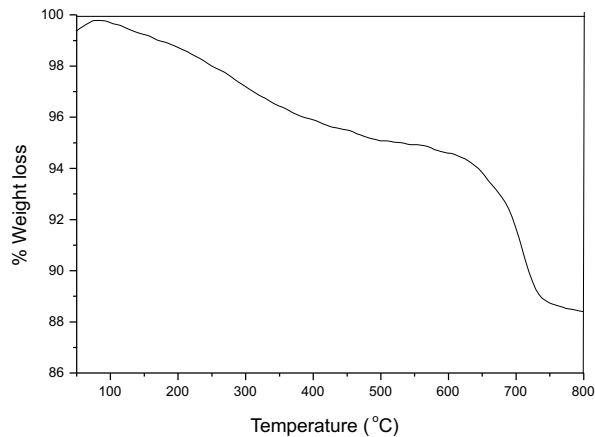


Fig. 7. TGA curve of the zinc aluminate (oxalate route) precursor.

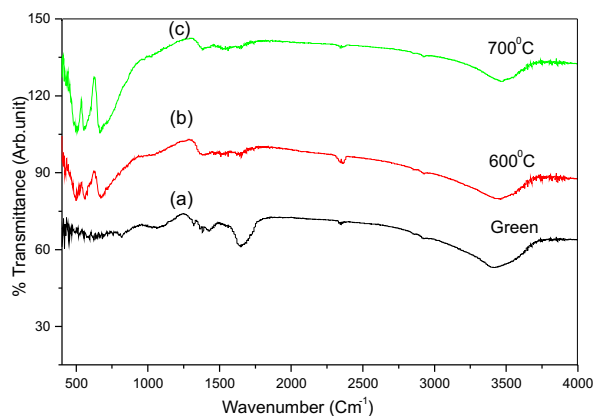


Fig. 8. FTIR spectra of zinc aluminate (oxalate route) a) uncalcined, b) calcined at 600 °C and c) 700 °C.

3.3. Malate Precursor Method

The XRD patterns of green and calcined powders synthesized via malate routes are shown in Fig. 9. The XRD pattern reveals that the green powder synthesized was amorphous in nature while after calcination at 600 °C single phase zinc aluminate was formed. The powder data are in agreement with JCPDS 05-0669. The average crystallite size was calculated as 22 nm. The FESEM picture shows the same type of morphology as for the tartrate and oxalate systems.

Fig. 10 shows the TGA curve of the green synthesized powder up to 1000 °C at a heating rate of 10 °C/min. TGA of the green powder shows a

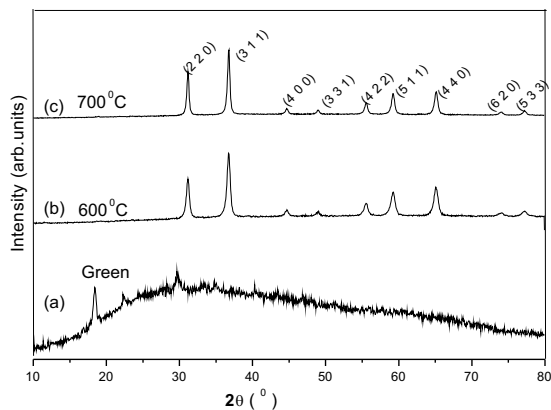


Fig. 9. XRD of the zinc aluminate powder (malate route) a) uncalcined, b) calcined at 600 °C and c) 700 °C.

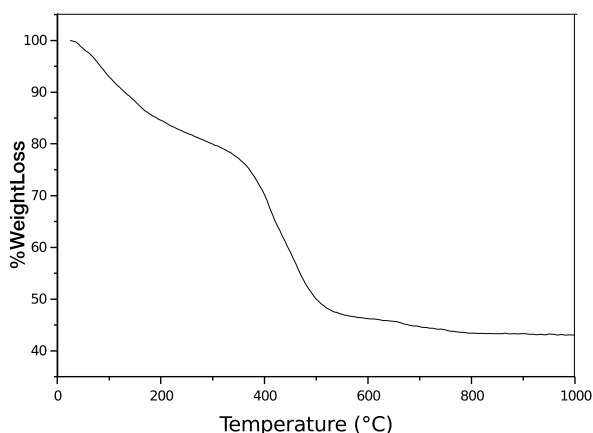


Fig. 10. TGA curve of the zinc aluminate precursor (malate route).

steady loss in weight up to 370 °C (25 %) which may be due to the presence of trapped nitrates, moisture and entrapped water. A sharp weight loss is observed from 370 °C to 500 °C (28 %) which may be due to the residual carboxylate and unburned carbon. No weight loss was observed above 600 °C indicating the formation of phase pure powder.

FTIR absorption spectra of green and calcined powder are shown in Fig. 11. Very small amount of impurities are found in green states which, as started earlier, is due to the absorption of O–H [3438 cm^{-1}] stretching vibration of the lattice water molecule, bending mode of H–O–H [1629 cm^{-1}] vibration, C=O [1320–

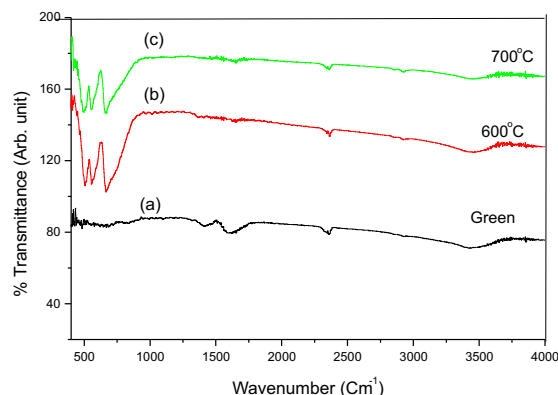


Fig. 11. FTIR spectrum of zinc aluminate (malate route) a) uncalcined, b) calcined at 600 °C and c) 700 °C.

1400 cm^{-1}] and O–C [1085 cm^{-1}] of coordinated COOH [18–20]. The sharp peaks of AlO_6 [660 and 550 cm^{-1}] are also observed when the powders are calcined at higher temperature. BET surface area of the synthesized powder was observed as 27.07 m^2/g .

4. Discussion

The mechanism of formation of zincaluminate by tartarate route may be similar to that of zinc-iron-citrate and zinc-iron-tartarate precursor route [22–24]. However in our case, instead of gel formation followed by calcinations/autoignition, partial oxidation of the complexes occurred during the evaporation process in presence of nitric acid. Since tartaric acid is also α -hydroxy acid, metal complexes are formed here as in Pechini's method [23]. The partial oxidation during evaporation generates hydroxo, hydroxo-carbonate phases as shown in our earlier work [24]. The presence of such phases is also supported by IR spectra. The TGA and IR studies shows the removal of extra absorbed water, hydroxo species and complete decomposition of organics up to 700 °C leading to the formation of single phase zinc aluminate.

In the case of oxalic acid and malic acid, the mechanism is a little bit different. Here the $\text{Zn}_3[\text{Al}(\text{ox})_3]_2 / \text{Zn}_3[\text{Al}(\text{Mal})_3]_2$ precursor formed by chelation decomposes in the presence of HNO_3

which on calcination gives rise to the product [25]. As oxalic acid and tartaric acid, are stronger ligands than malic acid, zinc tartarate, aluminium tartarate and zinc aluminoxalate complexes decompose at higher temperature in comparison to zinc-aluminomalate complex. This may be the reason of formation of zinc aluminate at lower temperature compared to other organic acids. The methods described above make it possible to obtain the nano-sized zinc aluminate at much lower temperature and shorter time than by the conventional ceramic methods.

5. Conclusion

This study describes a simple low temperature synthesis route for synthesizing ZnAl_2O_4 nanopowders using a solution evaporation method. Compared to the conventional solid-state reaction process and co-precipitation method, phase pure nanosized ZnAl_2O_4 can be formed at a much lower temperature through the tartarate, oxalate and malate precursor route. Furthermore the oxidation of zinc aluminate precursor by HNO_3 was accompanied by the evolution of CO_2 , NO_2 and water vapour which resulted in uniform size and morphology of the particle. Malic acid being the weakest ligand produces zinc aluminate at the lowest temperature compared to other acids. Organic acid and nitric acid present in the solution play a key role in the synthesis of ZnAl_2O_4 at a low temperature.

Acknowledgements

The financial support of the CSIR Supra Institutional Project SIP0023 is gratefully acknowledged.

References

- [1] SAMPATH S.K., KANHERE D.G., PANDEY R., *J. Phys. Condens. Matt.*, 11 (1999), 3635.
- [2] MATHUR S., VEITH M., HAAS M., HAOSHEN., LECERJ N., HUCH V., *J. Am. Ceram. Soc.*, 84 (2001), 1921.
- [3] CORDORO J.F., US Patent No. 6099637 (2000).
- [4] CORDORO J.F., ET AL., US Patent No. 5807909 (1998).
- [5] SHIOYAMA T.K., US Patent 4260845 (1981).
- [6] PELIER F., CHAUMETTE P., SAUSSEY J., BETTAHAR M.M., LAVALLEY J.C., *Mol. Catal. A. Chemical*, 122 (1997), 131.
- [7] SZYMANSKY R., TRAVERS CH., CHAUMETTE P., COURTY PH., DURAND D., In: DELMON B., GRANGE P., JACOBS P.A., PONCELET G., (ed) *Studies in Surface Science and Catalysis*, Elsevier, Amsterdam 31 (1987), 739.
- [8] COBB L.R., US Patent 4568784 (1985).
- [9] ROESKY R., WEIGUNY J., BESTGEN H., DINGERDISSEN U., *Appl. Catal. A: General*, 176 (1999), 213.
- [10] WELCH M.B., US Patent 4692430 (1986).
- [11] ESCARDINO A., AMORÓS J.L., GOZALBO A., ORTS M.J., MORENO A., *J. Am. Ceram. Soc.*, 83 (2000), 2938.
- [12] HONG W.S., DE JONGHE L.C., *J. Am. Ceram. Soc.*, 78 (1995), 3217.
- [13] KURIHARA L.K., SUIB S.L., *Chem. Mater.*, 5 (1993), 609.
- [14] CHEN Z., SHI E., ZHENG Y., LI W., WU N., ZHONG W., *Mater. Lett.*, 6 (2002), 601.
- [15] GIANNAKAS A.E., VAIMAKIS T.C., LADAVOS A.K., TRIKALITIS P.N., POMONIS P.J., *J. Colloid Interface Sci.*, 259 (2003), 244.
- [16] FANG G., LI D., YAO B.L., *J. Crystal growth*, 247 (2003), 393.
- [17] VALENZUELA M.A., JACOBS J.P., BOSCH P., REIJE S., ZAPATA B., BRONGERSMA H.H., *Appl. Catal. A: General*, 148 (1997), 315.
- [18] NAKAMOTO K., *Infrared and Raman Spectra of Inorganic and Coordination Compounds*, Part B, 5th ed:70, 75 (1997), John Wiley & Sons Inc.
- [19] SINGH V., CHAKRADHAR R.P.S., RAOC J.L., KIM D-K., *J. Solid State Chem.*, 180 (2007), 2067.
- [20] GHOSH S., DASGUPTA S., SEN A., MAITI H.S., *Mater. Res. Bull.*, 40 (2005), 2073.
- [21] WEI X., CHEN D., *Mater. Lett.*, 60 (2006), 823.
- [22] KUNDU A., ANAND S., VERMA H.C., *Powder Tech.*, 132 (2003), 131.
- [23] GUIATA F.J., BELTRAN H., CORDONCILLO E., CARDA J.B., ESCRIBANO P., *J. Eur. Ceram. Soc.*, 19 (1999), 363.
- [24] GHOSH S., SEAL A., DASGUPTA S., SEN A., MAITI H.S., *Proc. Int. Symp. on Advanced Materials and proceedings*, (ed), ADHIKARI B., BANNERGEE H., BANTHIA A.K., BASU S., BHARGAVA P., JACOB C., RAM S. *Material Science centre*, I.I.T, Kharagpur (2004), 1567–1574.
- [25] RANDHAWA B.S., *J. Mater. Chem.*, 10 (2000), 2847.

Received 05.05.2010

Accepted 12.09.2011